Publication Date: 15 May 2024
Archs Sci. (2024) Volume 74, Issue 2 Pages 226-232, Paper ID 2024230.
https://doi.org/10.62227/as/74230

The Impact of Near Third-air Pulverised Coal on NOx in NST-type Decomposition Furnaces is Studied Numerically

Siyuan Ding[1], Yanyong Qi[1,*], Shengqiang Ke[2] and Yulei Gao[3]
[1]School of Materials and Chemistry, Southwest University of Science and Technology, Mianyang 621000, China.
[2]Mianyang Qinuo New Material Development Co., Ltd., Mianyang 621000, China.
[3]Mianyan Polytechnic.

Corresponding authors: Yanyong Qi (e-mail:1227615020@qq.com).

Abstract In this study, the effects of nearly three-wind pulverised coal sprayed into the decomposition furnace on the temperature and NO distribution were analysed using the numerical simulation method of Computational Fluid Dynamics (CFD) for the nitrogen oxides (NOx) emission problem of NST-type decomposition furnace in a cement production line in a particular place. By creating a geometric model and meshing the decomposition furnace, as well as by using the proper mathematical models and numerical solutions, the trajectory, temperature distribution, and NO formation of coal dust were all simulated. The findings indicate that the three winds and the kiln tail flue gas have an impact on the motion trajectory of the coal dust after it is sprayed into the decomposition furnace, which causes a localised high temperature phenomenon to arise. The pulverised coal's trajectories varied according to the placements of the coal injection pipe, which in turn had an impact on the decomposition furnace's temperature distribution. Furthermore, NO is produced by the quick combustion of pulverised coal with a high oxygen content upon injection, which aggravates the development of a localised high temperature zone. Additionally, it was discovered that a higher fraction of coal infusion would highlight the unequal distribution of NO within the decomposition furnace. To sum up, this research offers a valuable resource and theoretical backing for addressing NO emission issues in decomposition furnaces.

Index Terms numerical simulation, decomposition furnace, pulverized coal injection, NOx, NOx emission

I. Introduction

AS the central piece of machinery in the new dry-process cement production technology, the decomposition furnace's internal operating condition directly influences the creation of clinker; it is primarily utilised to break down raw materials through pollutant emissions [1]. The primary component of the raw material is calcium carbonate, and exothermic coal burning provides the majority of the heat needed for the material to break down into calcium oxide. Nitrogen oxides (NOx), also known as NO_2, N_2O, and other oxides of nitrogen, are released during the burning of coal. decomposition furnace temperature is generally 850 1000 °C, only consider the generation of fuel-type NOx, high temperature type and fast-type NOx generation can be ignored, in addition, NO_2 is usually produced in the combustion process at less than 850 °C, so the decomposition of the furnace within the NOx is mainly NO [2]. As a result of the high temperature, large volume, and numerous complex chemical reactions present in the decomposition furnace during actual production, traditional thermal inspection methods are unable to thoroughly investigate the internal flow field of the furnace or the composition of each gas. In contrast, Computational Fluid Dynamics (CFD) is based on classical fluid dynamics and numerical computation methods based on the science of both theoretical and practical characteristics, offering The trajectories of the final three pulverised coal have moved towards the side walls in the central section of the decomposition furnace [3].

The formation of fuel-based NO_X, the relative position of the coal injection pipe, and the three winds of the various all depend on the concentration of O_2, which in turn affects the distribution of oxygen concentrations [4]. In order to address this issue, this paper uses a CFD numerical calculation method to alter the amount of coal dust near the three winds of the coal spraying area in order to study the impact of the decomposition furnace near the three winds on temperature and NO distribution. A site thermal calibration process found that in a place near the three winds at the coal pipe, there is a local high temperature phenomenon and NOX reached 1100 ppm.

II. Modeling and Numerical Solutions

A. Geometric modeling and meshing

Using software for three-dimensional modelling Solid is working on a cement 4800t/d NST decomposition furnace for 1:1 modelling [5]. The furnace is approximately 44.9 metres tall overall, with a 7.5-meter-diameter column. The diameter of the kiln end flue gas inlet is 2.4 metres, the diameter of the three air inlets is 2.8 metres, and the decomposition furnace outlet is 5.1 metres. Two symmetrically distributed discharging pipes are located in the centre of the decomposition furnace, with a diameter of 0.9 metres. Four coal injection pipes are situated between the three raw material and air discharging pipes, with a diameter of 0.2 metres. Four coal injection pipes, each with a diameter of 0.2 metres, are situated between the raw material discharge pipe and the three winds. The pipelines have a diameter of 0.9 metres [6].

The decomposition furnace is meshed using the ICEM-CFD programme, and the computational domain is linked and partitioned. Structured and unstructured mesh are the two categories of mesh. The simpler main component uses structured mesh with more precision, while the more complex decomposition furnace cone part, which carries the majority of the chemical processes, uses unstructured mesh, such as the burning of pulverised coal and raw material degradation. Local encryption combined with O-cut maximises mesh quality(see Figure 1). Both the structured and unstructured meshes have quality levels above 0.7 and 0.4, respectively. There are 2.23 million meshes in the model overall, and they are of good quality [7].

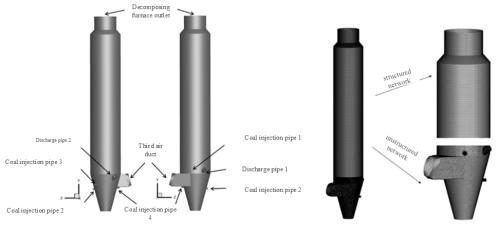

Figure 1: Decomposition furnace meshing and geometric model

B. Mathematical model

The radiation model was selected as the P1 model with a short computation time and solid particles and fluid gas-phase heat transfer; the turbulence model was chosen as the standard k-ε model with high applicability and accuracy for engineering calculations; the finite-rate/vortex dissipation model was used to calculate the gas-phase components of the reaction process under the component transport model; the pulverised coal was used as a discrete phase to enter the decomposition furnace [8]. Coal powder's particle size distribution followed the rosin-rammler distribution, with a minimum of 1 μm, a maximum of 92.6 μm, an average of 21.12 μm, a dispersion coefficient of 4.3, and the particle agglomeration model chosen as the Standard model [9].

The combustion process of pulverised coal is typically separated into two phases: fixed carbon combustion and volatile precipitation [10]. While fixed carbon is burned in a kinetic/diffusion-controlled reaction that yields CO as the result, volatiles are precipitated using a two-rate competitive reaction that splits the volatiles into CH_4 and CO. CO and CH_4 eventually experience an oxidation process.

The fuel-type NOX generation model is adopted by the NOX generation model for pollutants, and Figure 2 illustrates the NOX generation process offered in Fluent. Fuel-type NOX makes up the great bulk of NOX in the decomposer.

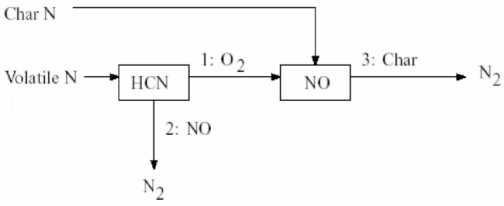

Figure 2: Fuel-based NOx generation pathway

C. Numerical solution

The finite volume approach discretizes the governing equations of the fluid phases, and the second-order windward differential format is used to generate the discrete equations as a system of differential equations. The SIMPLE method with low relaxation factor is utilised to solve the discrete system of equations pertaining to pressure and velocity coupling. The near-wall region is handled using the conventional wall function, and a no-slip wall is utilised. For the energy equation term and the P1 radiation term, the residual convergence conditions are fewer than 10^{-6}; for the remaining residuals, they are less than 10^{-3}.

D. Boundary condition setting

The boundary conditions used in this study are the measured and calculated values of the thermal calibration of the plant's decomposition furnace, and the kiln conditions were stable during the calibration period. The raw material feeding quantity is 417t/h, clinker production is 6400t/h, the total amount of coal feeding at the end of the kiln is 21.6t/h, and the amount of coal sprayed by each coal pipe depends on the proportion of the total amount of coal sprayed by the coal pipe , as shown in Table 1.The working air volume of three times is 604464m^3/h, the working air volume of kiln end flue gas is 429331m^3/h, the working air volume of the coal feeding air is 10935m^3/h, and the Table 2 shows the working air volume of the calcining furnace. Boundary condition setting.(see Table 1 ,Table 2, 3 and 4)

The industrial and elemental analyses of coal dust are shown in Table 3 and 4.

III. Numerical simulation results

Table 1: Pulverized coal consumption at different coal injection ratios

Coal injection ratio(%)	Coal injection tube(1)(kg/s)	Coal injection tube (2)(kg/s)	Coal injection tube(3)(kg/s)	Coal injection tube (4)(kg/s)
0	0.001	2.007	2.007	2.007
10	0.602	1.806	1.806	1.806
40	2.408	1.204	1.204	1.204
65	3.913	0.702	0.702	0.702

Table 2: Calciner boundary conditions

Placement	Boundary condition	Speed(m/s)	Mass flow rate(kg/s)	Temperature(K)	Pressure (Pa)	Hydraulic diameter(m)
Kiln exhaust gas	Velocity inlet	26.38	/	1401	-180	2.4
Third air duct	Velocity inlet	27.18	/	1253	-250	2.8
Tremie pipe1	Velocity inlet	/	40.72	1053	/	0.9
Tremie pipe2	Velocity inlet	/	40.72	1053	/	0.9
Decomposing furnace outlet	Pressure output	/	/	1143	-700	5.1

Table 3: Industrial analysis of pulverized coal

	Ash content	Fixed carbon	Volatile	Moisture content	Lower calorific valuekJ/kg
Mass(%)	15.23	52.79	30.43	1.55	25120

Table 4: Element analysis of pulverized coal

	C	H	O	N	S
Content(%)	76.71	5.58	15.76	1.42	0.53

A. Kinematic trajectory

In Figure 3, the temperature is represented by the colouring depth of the three wind and coal particle traces. When the three unidirectional winds enter the decomposition furnace horizontally and are compressed by the flue gas at the end of the kiln, they move in the shape of a spiral rise. At the height of the decomposition furnace, which is between 10 and 20 metres, the colouring turns red to illustrate the phenomenon of the high temperature in the area. The coal dust follows distinct trajectories due to the disparate relative positions of the three air pipes and the coal injection pipe. In the decomposition furnace, after entering the high temperature of the three winds carried by the intense combustion of high concentrations of O_2 reaction, a localised high temperature phenomenon emerged. In the field, temperature measurements at the coal injection point 1 showed extremely high temperatures and even burned out thermocouples. Coal injection pipe1,2, 3, 4, sprayed coal dust.

This coal dust was near the three wind pipe. backed up the simulation's findings. Coal dust 2 and 3 positions are somewhat remote from the three wind pipes. The trajectory of the decomposition furnace's lower part is primarily influenced by the upward movement of the kiln exhaust flue gas, while the middle and upper parts of the column are affected by the upward movement of the kiln exhaust flue gas, which carries upward coal dust as well as the spiral upward of the three winds to meet, collision, and disperse of the three winds [11]. A portion of the coal dust is caused by the three winds spiralling upward and a portion is caused by the kiln tail flue gas coercing upward movement [12]. Coal injection pipe12 is also near the three wind pipes, but it is not in the three winds in the region's mainstream movement.

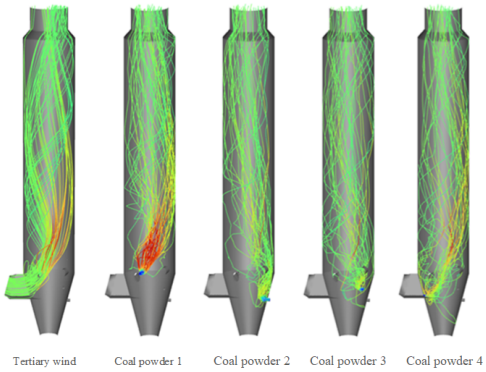

Figure 3: Tertiary wind trace and pulverized coal particle trajectory

B. Temperature field

The decomposer's temperature rises due to the proximity of coal powder1 to the third air duct. The amount of coal sprayed has an impact on both the decomposer's temperature and the dispersion of NOx. The temperature cloud produced by varying percentages of the total amount of coal 1 is displayed in Figure 4. The high temperature region of the decomposer is growing as the proportion of coal injection pipe1 progressively rises from 0% to 65%. This expansion is shown by the expansion of the high temperature region along the height of the decomposer in both the longitudinal direction and the transverse cross-section. This is where the coal dust from the coal spray pipe1 into the decomposition furnace after the main movement area is clearly visible in the proportion of 65% of the three air ducts above the side of the high-temperature area. The coal spray pipe1 and the three air ducts are located very close to the location of the high concentration of oxygen and

the rapid combustion of coal dust at high temperatures. As a result of the increase in coal dust, heat builds up in this area. Decrease the amount of coal dust in the coal spray pipe1, localized Reduce the amount of coal dust in the coal injection pipe1, the local high temperature phenomenon is obviously relieved [12].

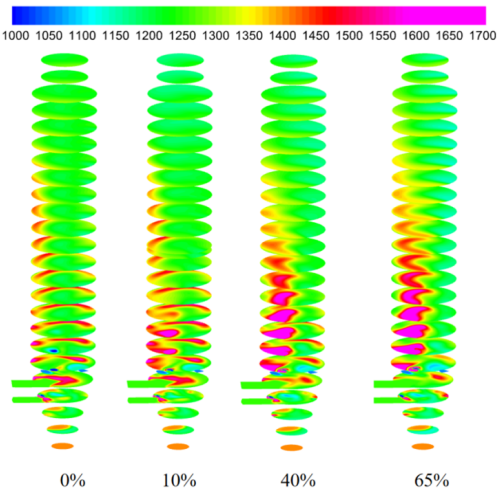

Figure 4: Temperature cloud for different coal injection ratios (K)

Examine the primary high-temperature area cross-sections 6, 7, and 8. When the proportion of coal dust 1 is zero, the high-temperature area is primarily concentrated in the back side, and the size of the high-temperature area in the back side of the nozzle1 and the proportion of coal spraying exhibit a "negative correlation": as the proportion of coal spraying increases, the high-temperature area progressively decreases, suggesting that this area is primarily for the pulverised coal motion of nozzles 2, 3, and 4 Figure 5. The coal powder 1 movement track is positioned in the "triangular" section at the front [13], [14].

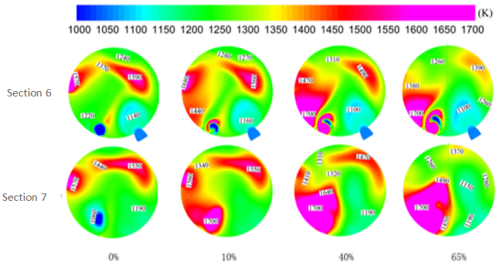

Figure 5: Temperature distribution of sections 6 and 7

Figure 6 illustrates that in the decomposition furnace height of 0–9 m, the proportion of coal injection has very little effect on temperature; in various coal injection conditions, the temperature curve is consistent and fluctuates little; the kiln end flue gas is the main source of temperature variation; in the 9–20 m interval, however, a significant difference is shown: the proportion of coal injection of 0% of this condition of average temperature rise is not large, peaking at 14 m; The total amount of coal sprayed did not change over the 9–20 m interval, but the amount of coal dust in the nozzle 1 greatly affects the average temperature of the decomposition furnace. For every 1 unit of pulverised coal in the nozzle, the average temperature of the decomposition furnace will increase by 1.5 times or decrease by 2.5 times. The average temperatures of the decomposition furnace were 1284K, 1331K, 1379K, and 1367K, respectively, as the quantity of pulverised coal increased [15], [16].

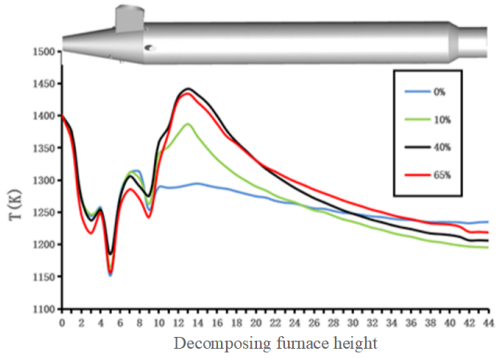

Figure 6: Average temperatures at different heights of the decomposition furnace (K)

C. NOx generation and distribution

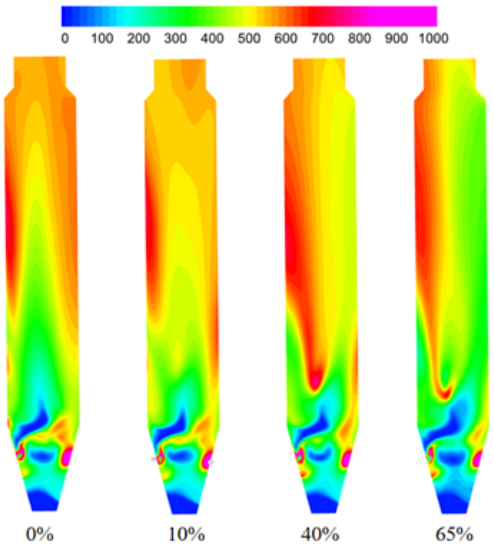

Figure 7: Distribution of NO (ppm) for different coal injection ratios in X=0 cross section

The cross-section of X = 0 in Figure 7 shows that, under various coal injection ratio conditions, the overall trend of the NO distribution remains consistent. This suggests that, while the proportion of coal injection pipe ranges from 0% to 65% of the interval, the flow field in the decomposition

furnace is not more affected by an increase in the proportion of coal injection. This is because high-speed bottom-up flow of hot flue gas, rapid combustion, and upward movement quickly wrap the coal powder from the coal pipe into the decomposition furnace. It is evident that the colour of the low value area in the decomposer cone deepens as the proportion of coal injection increases, suggesting that coal dust 1 has a negligible effect on the formation of NO in this location. The two areas near nozzles 1 and 2, respectively, where pulverised coal meets with a high concentration of oxygen and burns quickly to produce a large amount of combustion-type NO, and the dark blue "lightning-type" low NO value area near nozzle 1, where there is very little pulverised coal and raw material, are the causes of the high NO value of 1200 ppm on both sides of the cone. The dark blue "lightning-type" NO low value area close to the nozzle1 is the same. A portion of the NO is unequally distributed between the left and right sides in the decomposer column, with the left side having a value of about 800 ppm. The characteristic of uneven distribution becomes more evident when the coal injection ratio is increased from 0% to 65%. The high NO value area on the right side vanishes and the high value area on the left side increases as the proportion of coal injection increases.

Figure 8 shows the distribution of NO (ppm) for different coal injection ratios for the Z=0 cross section.

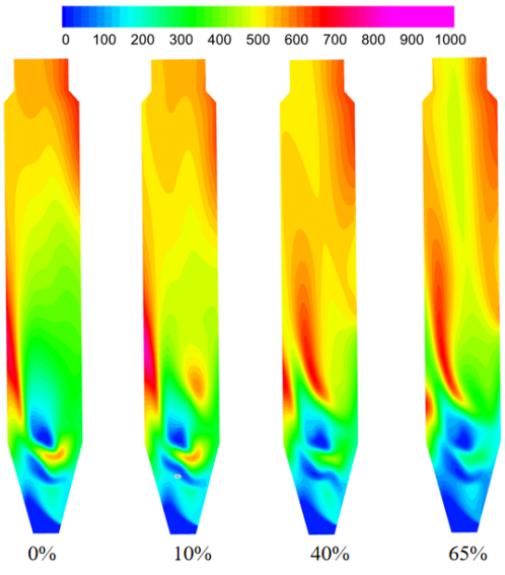

Figure 8: Distribution diagram of NO (ppm) at different coal injection ratios for section Z=0

Figure 8 shows that, under various operating conditions, the centre "square" NO low value area in the cross-section of Z=0 is the contour of a high-speed tertiary wind entering the decomposition furnace transversely at Z=0, where essentially no NO is formed and less fuel is required. The left side of the decomposition furnace has a greater NO distribution, reaching 800 ppm at a height of 13 to 20 m. The distribution of NO at the decomposition furnace's outflow varies significantly as well, with the right side wall having a higher concentration of NO.

Determining the high value area of the NO distribution is crucial for precise denitrification of the cement decomposition furnace. The location of the NO high value area has been established in the content above. At this point, we will concentrate on the NO high value area and the decomposition furnace's exit, examining their relationship to variations in the amount of pulverised coal.

Taking Y=11m and Y=17m with the exit of the decomposer for the study Figure 9 shows the distribution of NO (ppm) for different coal injection ratios in the Y=11 section.

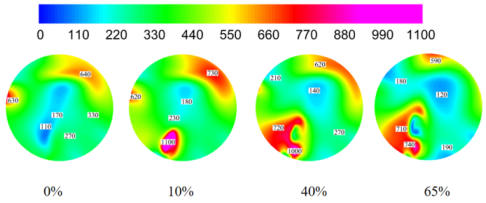

Figure 9: Distribution diagram of NO (ppm) at different coal injection ratios for dection Y=11

According to Figure 10, the Y=11 cross-section shows that the two conditions of 10% and 40% coal injection have the highest NO, with the NO value of the two conditions reaching 1000 ppm in the lower right; the condition of 65% coal injection also exhibits a wide range of low NO values, with the exception of 740 ppm NO aggregation in the lower right region; the NO distribution is less in this cross-section of 0% coal injection. The coal injection ratio in this section is 0%, and the NO distribution is modest in this instance. The NO distribution in this plane is highly variable, ranging from a high of 1100 ppm to a low of 100 ppm. The pulverised coal 1 has a significant effect on the formation of NO in this plane. From low to high, the average NO (ppm) of the coal injection ratio is 305, 353, 369, and 299, in that order.(see Figure 10)

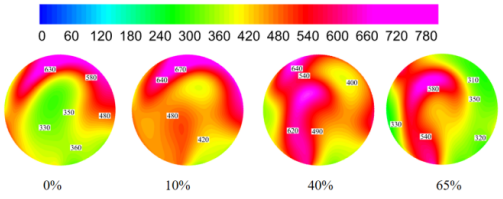

Figure 10: Distribution diagram of NO (ppm) at different coal injection ratios for section Y=17

Under these two conditions, the low value area of NO distribution of 0% coincides with the high value area of NO distribution of 65%, and vice versa; thus, it can be known that the main movement range of the coal powder1 in this cross-section, in other words, in the low value area of NO distribution of 0% of the coal spraying ratio, the NO generation is dominated by the coal powder1.

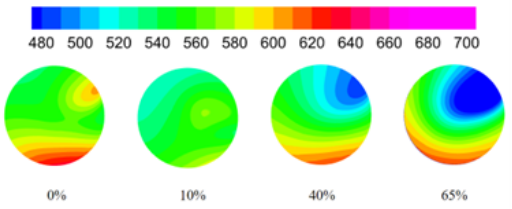

Figure 11: Distribution diagram of NO (ppm) at different coal injection ratios for section Y=17

As can be seen in Figure 11 at the outlet of the decomposer, the distribution of NO shows a different phenomenon from the previous two. With the increase of the proportion of coal injection: the distribution of NO is 0%>10%>40%>65% are 567ppm, 550ppm, 541ppm, 525ppm, respectively. where the coal powder 1 the proportion of coal injection is 10% of the decomposition furnace outlet NO distribution is uniform, while in the other conditions NO distribution is not uniform.

The pulverised coal 1 through the coal injection pipe 1 into the decomposition furnace will be rapidly combusted with high temperature and high concentration of oxygen, generating a large number of fuel-type NO. The decomposition furnace 8m–18m of this interval of the pulverised coal 1 dominated the distribution of NO in this area, as can be seen from the figure, where the 0% up to 10% of the average value of NO is accounted for. This is the reason for the above situation. There is a noticeable increase in the average value of NO. And after the coal dust 1 for the impact of NO is slowly weakened, this is because the remaining three coal nozzle location from the three winds farther away, three winds into the decomposition furnace trajectory for the spiral upward movement, means that the remaining three coal dust can not be like coal dust 1 as the first time to meet with the three winds, combustion. Rather, with the kiln end flue gas upward diffusion of part of the distance before a large number of three winds with the convergence, combustion occurs to generate fuel-type NO. The remaining three nozzle compared to the nozzle1, relatively more lagging, nozzle 1 pulverized coal trajectory in the center of the furnace mainly in the decomposition of the track, the remaining three pulverized coal trajectory is closer to the side wall, which is led to the previous distribution of NO distribution of the main reason.(see Figure 12).

IV. Conclusion

The movement trajectory of coal dust near the three wind pipes is mainly affected by the three winds. Coal powder1 is wrapped by the three winds, and its trajectory is mainly in the center of the decomposition furnace, while the trajectory of the remaining three coal powder is closer to the side wall.

There are local high temperature and 1000ppm NO high value area in the near three air ducts coal spraying area in the field measurement and calculation simulation.

The average temperature of the decomposer outlet is: coal injection ratio 0% (1234K)> coal injection ratio 65% (1219)>

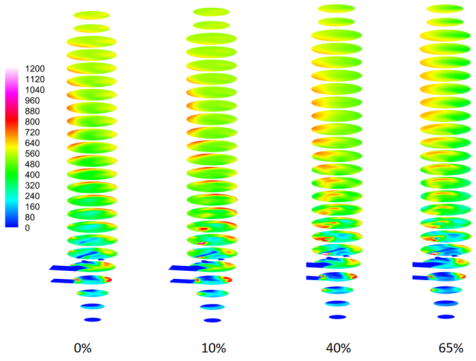

Figure 12: Distribution of NO(ppm)at different coal injection ratios

coal injection ratio 40% (1206K) > coal injection ratio 10% (1195K); with the increase in the proportion of coal injection: the decomposer outlet NO distribution of 0% > 10% > 40% > 65% were 567ppm, 550ppm, 541ppm, 525ppm.

The height of the decomposer from 8m to 18m, the coal dust 1 dominates the NO distribution in this area, and a small increase of coal dust 1 in this area will also cause a more obvious rise in NO.

Funding

There is no funding support for this study.

References

[1] Jeon, M., Lee, E., Kim, M., Jegal, H., Park, S., Chi, J. H., ... & Keel, S. I. (2023). Nitric oxide (NO) and nitrous oxide (N2O) emissions during selective non-catalytic reduction and selective catalytic reduction processes in a pulverized coal/Ammonia Co-fired boiler. *Journal of Environmental Chemical Engineering, 11*(2), 109398.

[2] Go, E. S., Kim, H. W., Kang, S. Y., Keel, S. I., Ling, J. L. J., & Lee, S. H. (2022). Analysis of combustion characteristics using CPFD in 0.1 MWth oxy-fuel CFB. *International Journal of Nanotechnology, 19*(1), 63-74.

[3] Buku, A., Salu, S., Pangadongan, M., & Bia, J. B. (2022, December). Analysis of Tensile Tests and Microstructures of ST. 37 Steel Undergoing Carburizing Process Using Coal Powder. In *Journal of Physics: Conference Series* (Vol. 2394, No. 1, p. 012039). IOP Publishing.

[4] Ali, M. M., Ali, M. L., Rakib, M. R. J., Islam, M. S., Habib, A., Hossen, S., ... & Phoungthong, K. (2022). Contamination and ecological risk assessment of heavy metals in water and sediment from hubs of fish resource river in a developing country. *Toxin Reviews, 41*(4), 1253-1268.

[5] Jo, H., Park, J., Kang, W., Hong, J., Yoon, S., Ra, H., & Ryu, C. (2021). Influence of Uneven Secondary Air Supply and Burner Tilt on Flow Pattern, Heat Transfer, and NOx Emissions in a 500 MWe Tangential-Firing Coal Boiler. *Energies, 14*(24), 8352.

[6] Zhao, J., Wang, X., Tian, Z., Deng, H., Jiang, Z.,& Li, Y. (2024). Optimization Design and Evaluation of the Industrial Distillation-Membrane Separation Process. *Chemical Engineering & Technology, 47*(2), 335-348.

[7] Liu, J., Ma, T., Chen, J., Peng, X., Zhang, Y., Wang, Y., ... & Gao, J. (2024). Insights into PM2. 5 pollution of four small and medium-sized cities in Chinese representative regions: Chemical compositions, sources and health risks. *Science of The Total Environment,* 170620.

[8] Khan, M. A. U., & Paul, A. (2021). Brick Kiln's Green House Gas (GHG) emission and public health perspectives: A study in Chattogram, Bangladesh. *Bangladesh J. Environ. Res, 12,* 50-61.

[9] Jamsran, N., Park, H., Lee, J., Oh, S., Kim, C., Lee, Y., & Kang, K. (2021). Influence of syngas composition on combustion and emissions in a homogeneous charge compression ignition engine. *Fuel, 306,* 121774.

[10] Yun, J. G., Kim, J. Y., Lee, H. M., Baik, G. Y., Jeon, M. K., Yun, J. H., & Hong, J. G. (2022). A study on the N2O reduction rate according to

temperature and residence time in the exhaust gas atmosphere emitted on combustion of air and oxygen. *ACS omega, 7*(4), 3434-3441.

[11] Sanchez, P. D. C., Aspe, M. M. T., & Sindol, K. N. (2022). An overview on the production of bio-briquettes from agricultural wastes: methods, processes, and quality. *Journal of Agricultural and Food Engineering, 1,* 0036.

[12] Go, E. S., Kim, H. W., Kang, S. Y., Keel, S. I., Ling, J. L. J., & Lee, S. H. (2022). Analysis of combustion characteristics using CPFD in 0.1 MWth oxy-fuel CFB. *International Journal of Nanotechnology, 19*(1), 63-74.

[13] Nguyen, H. K., Moon, J. H., Jo, S. H., Park, S. J., Bae, D. H., Seo, M. W., ... & Song, B. (2021). Ash characteristics of oxy-biomass combustion in a circulating fluidized bed with kaolin addition. *Energy, 230,* 120871.

[14] Zhou, J., Liu, Q., Jiang, Q., Ren, W., Lam, K. M., & Zhang, W. (2023). Underwater camera: Improving visual perception via adaptive dark pixel prior and color correction. *International Journal of Computer Vision,* 1-19.

[15] Zhou, J., Li, B., Zhang, D., Yuan, J., Zhang, W., Cai, Z., & Shi, J. (2023). UGIF-Net: An efficient fully guided information flow network for underwater image enhancement. *IEEE Transactions on Geoscience and Remote Sensing, 61*, 1-17.

[16] Dong, Q.,& Liu, X. Optimization Practice of University Innovation and Entrepreneurship Education Based on the Perspective of OBE. *Journal of Combinatorial Mathematics and Combinatorial Computing, 118*, 181-189.